Food and Bioprocess Technology manuscript No.
(will be inserted by the editor)

Artificial neural network assisted spectrophotometric method for monitoring fructo-oligosaccharides production

Balázs Erdős · Maarten Grachten · Peter Czermak · Zoltán Kovács

Received: date / Accepted: date

Abstract Short-chain fructo-oligosaccharides (FOS) are considered as low-calorie carbohydrates with prebiotic function. They can be produced from sucrose by fructosyltransferase activity, resulting in a mixture of saccharides with different chain lengths. Current practice for carbohydrate analysis involves the use of time-costly and off-line chromatographic procedures. This study is dedicated to the development of an artificial neural network (ANN) model for predicting carbohydrate composition from the direct measurement of UV spectra. A total of 182 samples were generated by operating an enzyme membrane reactor (EMR) under both optimal and suboptimal settings. The concentration data determined by HPLC and corresponding absorbance readings were used to train a two-layer feedforward neural network. The optimized network was

Balázs Erdős
Department of Food Engineering, Szent István University, Budapest, Hungary

Maarten Grachten
Department of Computational Perception, Johannes Kepler University, Linz, Austria

Peter Czermak
Institute of Bioprocess Engineering and Pharmaceutical Technology, University of Applied Sciences Mittelhessen, Giessen, Germany
Department of Chemical Engineering, Kansas State University, Manhattan, Kansas, USA
Fraunhofer Institute IME-Bioresources, Giessen, Germany

Zoltán Kovács
Department of Food Engineering, Szent István University, Budapest, Hungary
Tel.: + 36 1 305 7234, E-mail: kovacs.zoltan@etk.szie.hu

then validated by using new observations that were not involved in the training. The model explained 98, 97 and 88 percent of the variation in the composition of the new observations regarding the main components sucrose, kestose and glucose with a mean squared error of prediction of 6.59, 3.40 and 2.81, respectively. The results indicate that the proposed UV-ANN method has a great potential to be used for the real-time monitoring of the bioconversion.

Keywords fructo-oligosaccharides · enzyme membrane reactor · artificial neural network · UV spectrophotometry · prebiotics

1 Introduction

Food consumption tendencies show an increasing demand for products with enhanced composition that contribute to health improvements (Falguera et al, 2012). Fructo-oligosaccharides (FOS) are recognized as low-digestible carbohydrates with prebiotic attributes (Rastall, 2010). They may alter the colonic microflora toward a healthier composition, reduce constipation, and decrease the serum cholesterol level while supplying small amount of energy (Mutanda et al, 2014). FOS are usually added to dairy products, beverages and desserts (Bali et al, 2013).

FOS are fructans with a degree of polymerization up to 10 (Corradini et al, 2013). They naturally occur in biological materials, however, in low concentration (Dominguez et al, 2013). They are commonly manufactured either by the enzymatic hydrolysis of inulin (Nguyen et al, 2011; Sarup et al, 2016) or by transfructosylation from sucrose. In the latter case, short-chain FOS are generated by the activity of fructosyltransferase enzymes. The production processes may involve either whole cells or (partially) purified enzymes, in immobilized or free form (Kovács et al, 2014). The product of the enzymatic catalysis is usually a mixture of saccharides including fructosyl-nystose (GF4), nystose (GF3), kestose (GF2), glucose (G), fructose (F), and non-reacting sucrose (GF). Recently, continuous production techniques employing packed bed reactors (Tanriseven and Aslan, 2005; Ghazi et al, 2005; Chen et al, 2014), fluidized bed reactors (Lorenzoni et al, 2015), and enzyme membrane reactors with inert (Ur Rehman et al, 2016) and

catalytic membranes (Nishizawa et al, 2000; Hicke et al, 2006) have received considerable attention. In contrast with a conventional batch process utilizing soluble enzymes in a stirred-tank reactor, these techniques allow the production of an enzyme-free product in a continuous manner by recovering the biocatalysts.

A wide range of analytical techniques have been proposed for the identification and quantification of FOS. Among them, high-performance liquid chromatography (HPLC) is the most prevalent method. Various HPLC setups are available, employing refractive index detectors (RID) (Petkova et al, 2014), evaporative light scattering detectors (ELSD) (Li et al, 2013), pulsed amperometric detectors (PAD) (Corradini et al, 2004), and pulsed electrochemical detection (PED) (Borromei et al, 2009). In combination with HPLC, matrix-assisted laser desorption/ionization time-of-flight mass spectrometry (MALDI-TOF-MS) is another highly selective technique for the determination of chain length distribution of FOS and inulin (Borromei et al, 2009). Although thin layer chromatography (TLC) represents an available option, it is known to be laborious and costly due to its chemical and material demand (Petkova and Denev, 2015). Similarly, gas chromatography (GC) is reported to be unfavorable since it requires time consuming sample preparation (Joye and Hoebregs, 2000). The application of Fourier transform infrared spectroscopy (FT-IR) and proton nuclear magnetic resonance (H NMR) spectroscopy to inulin analysis has also been investigated. FT-IR was used to quantify some crystalline fructans obtained from fermentation broth by precipitation (Grube et al, 2002), and H NMR was successfully applied to monitor acidic hydrolysis of inulin conducted in deuterium oxide (Barclay et al, 2012).

In industrial practice, continuous processes require a strict supervision in order to ensure a controlled and safe plant operation. HPLC, the standard procedure for saccharides analysis, is a sensitive and reproducible method, but it is time-costly, laborious, and requires expensive instrumentation and technically trained personnel. Since HPLC is an off-line technique, there is a considerable long delay between sampling from the production line at the facility and receiving information on the carbohydrate compo-

sition from the analytics lab. There is a need for robust, real-time methods to detect possible deviations from an optimal process behavior in FOS manufacturing.

Spectroscopic analysis in the ultraviolet-visible (UV/vis) spectral region is a common and simple method for acquiring information from sample solutions. Spectrophotometer setups equipped with optic fiber technology that allow on-line measurement are readily available on the market (Van Den Broeke et al, 2006). The complex nature of spectral data requires adequate data analysis tools, such as multivariate techniques and artificial neural networks (ANN). ANNs are considered as nonlinear statistical modeling tools capable of estimating complex functions. ANN models have found several applications in food engineering, biotechnology and related fields (e. g. (Mateo et al, 2011; Prabhu and Jayadeep, 2017; Lin et al, 2011; Cámara et al, 2010)).

Molecular spectroscopy represents a potential candidate for the rapid detection of carbohydrates. Dias et al (2009) have first shown that UV-spectroscopy combined with chemometrics methods, such as partial least-squares regression (PLSR) and artificial neural networks (ANN), could serve as a fast alternative method for monitoring of galacto-oligosaccharides (GOS) production. They have successfully constructed PLSR and ANN models trained on UV data to predict the concentration of two fractions (lactose and total GOS) in samples taken from fermentation broth. The chemical analytics of metabolites, that may appear in the matrix as a result of microbial activity and may interfere with UV readings, were not reported. The proposed method involved the filtration (for cell removal) and dilution of the samples prior to UV analysis of a total of 53 samples. Recently, Veloso et al (2012) have published a book chapter on UV spectrophotometry methods for dietary sugars. Based on some preliminary experiments, the authors point out that such methods might potentially be applied for monitoring the production of FOS in fermentative processes, given that real samples are used in the future to validate this hypothesis. To the best of our knowledge, this hypothesis has never been proven, and our study is the first of its kind to explore the applicability of UV spectroscopy for FOS monitoring in depth.

This study investigates artificial neural networks dedicated to the real-time quantification of FOS fractions to mono- and disaccharides concentrations based on UV spectral data. First, a large number of samples were generated by operating an enzyme membrane reactor (EMR). Concentrations of the individual saccharides fractions and UV spectra of the enzyme-free samples were determined by HPLC analysis and UV spectroscopy, respectively. Then, an artificial neural network model was trained to predict the concentration of saccharides in the samples based on their UV spectra. Finally, the optimized network was validated by using new observations, which were not included in the training data.

2 Materials and methods

2.1 Materials

Food-grade sucrose manufactured by 1. MCM Kft. (Kaposvár, Hungary) was purchased from a local food store. Pectinex Ultra SP-L, a commercial enzyme preparation from *Aspergillus aculeatus*, was supplied by Novozyme A/S (Bagsværd, Denmark). The reaction liquor, used in all the experiments, consisted of 40 w/w% food-grade sucrose in deionized water. Its pH was set to 5.7±0.2 with a 0.1 M HCl solution. A spiral-wound ultrafiltration (UF) membrane module with a filtration area of 0.37 m^2 and a cut-off of 20 kDa was purchased from Synder Filtration Inc. (San Francisco, USA).

2.2 Enzyme membrane reactor

The schematic drawing of the lab-scale EMR employed for generating samples is shown in Fig. 1.

The enzymatic catalysis took place in the stirred-tank reactor using soluble enzymes. The feed pump circulated the enzyme-containing reaction liquid through the UF module. The cross-flow rate of the pump was adjusted to 0.16 m^3h^{-1} with the frequency drive of the pump. The temperature of the solution was controlled by an external bath thermostat and kept at 50±0.5°C. The applied UF membrane completely

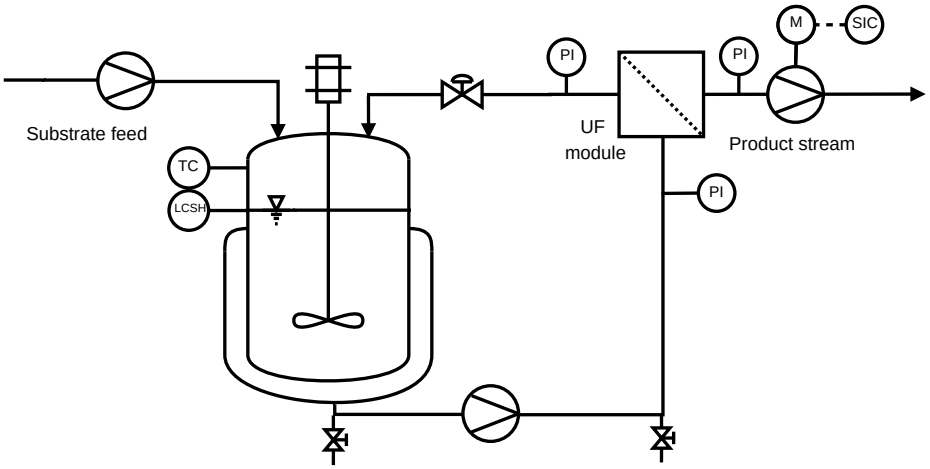

Fig. 1 Schematic drawing of the enzyme membrane reactor

rejected the enzymes but allowed the passage of carbohydrates. The retentate-side pressure was adjusted manually with the control-valve to 1 bar. The residence time (i. e. the ratio of reactor volume to product flow-rate) was kept constant during process runs. This was achieved by ensuring that the volumetric flow-rate of the permeate (i. e. product stream) is equal to that of the feed (i. e. supply stream of the fresh saccharose solution). For controlling the permeate flow-rate, a pump on the permeate-line was employed. The rotation of this pump was adjusted to the desired value to ensure a constant permeate flow-rate. An automatic filling of fresh saccharose solution to a constant volume was realized by employing a supply pump and a conductive level switch.

2.3 Sample preparation

Experimental samples containing mono-, di-, and oligomers in various concentrations were generated by operating the EMR in continuous fashion. Ten experimental runs were conducted by varying the enzyme load (i. e. the ratio of the mass of the enzyme to that of the solution) in the range of 5 to 50 $\mathrm{g\,kg^{-1}}$ and the residence time in the range of 1 to 4 h. The EMR was operated until steady-state was reached, typically for

6-8 hours. Samples were taken from the permeate at several time points during the process run-time.

2.4 Chemical analysis

Samples taken from the permeate were diluted with a dilution factor of 5 prior to HPLC analysis. An HPLC system by Thermo Fisher Scientific Inc. (Waltham, MA, USA) was used as reference method for carbohydrate analysis. It included an SCM1000 degasser, a P200 gradient pump, and an AS100 autosampler equipped with a built-in column thermostat. An RNM Carbohydrate 8% Na+ 300x7.8 (Phenomenex Inc., Torrance, USA) analytical column together with a guard column was used at 50°C at 0.2 mL min^{-1} with pre-filtered ($2\mu m$) DI water as mobile phase. Peak detection and integration was performed by a Shodex R-101 refractive index detector manufactured by Showa Denko Europe GmbH (Munich, Germany), an N2000 Chromatography Data System interface and a N2000 Photographic Data Workstation software package supplied by Science Technology Inc. (Hangzhou, China). The concentration of individual carbohydrate fractions was calculated by integrating the respective peak areas and then expressed in relative mass percentage. The relative mass percentage [%] is the ratio of the mass of a substance to the total mass of carbohydrates present in the solution multiplied by 100.

The UV spectrophotometry analysis was carried out with a Spectronic GENESYS 5 UV-Visible Spectrophotometer manufactured by Thermo Electron Corporation (Waltham, MA, USA). Absorbance of samples at 34 wavelengths, ranging from 201 to 300 nm, at intervals of 3 nm was measured without dilution at room temperature.

2.5 Artificial neural networks

The purpose of the present study is to predictively model the relationship between the UV absorbance measurements and the carbohydrate concentrations, as obtained by the

HPLC measurements, such that given a measurement of UV absorbances over different wavelengths, we can reliably predict the corresponding carbohydrate composition.

We use artificial neural networks (ANNs) for this modeling task. ANNs are non-linear models suitable for approximating complex scalar or vector-valued functions. They consist of information processing units that mimic the behavior of neuron cells in living organisms, in the sense that they output a non-linear response to a weighted sum of their inputs. These units are arranged into layers, where each unit receives information from all the units in the previous layer. The lowest layer of this network—receiving the input—is called the *input layer* $\mathbf{l}_1$, the highest layer—producing the output—is the *output layer* $\mathbf{l}_K$, and any intermediate layers are called *hidden layers* $\mathbf{l}_2, \cdots, \mathbf{l}_{K-1}$. Thus, given UV absorbances $\mathbf{x}_i$, an ANN approximates the relative mass percentage of the individual carbohydrate fractions $\mathbf{y}_i$ according to the following recursive equations:

$$\hat{\mathbf{y}}_i = \mathbf{l}_K \tag{1}$$

$$\mathbf{l}_k = f_k\left(\mathbf{W}_k^T \mathbf{l}_{k-1} + \mathbf{w}_k\right) \tag{2}$$

$$\mathbf{l}_1 = \mathbf{x}_i \tag{3}$$

where $\theta = \{\ \mathbf{W}_k, \mathbf{w}_k \mid k \in [2, K]\ \}$ are the parameters of the model, and f_k is a function applied elementwise to its arguments, i. e. the non-linear *sigmoid* function for hidden layers $(f_2, \cdots, f_{K-1})$, and in our case of real-valued output variables, the *identity* function for f_K.

In a procedure referred to as *training*, the model parameters are adjusted based on a set of data pairs $(\mathbf{x}_i, \mathbf{y}_i)$ $(i \in [1, N])$. More specifically, the optimal parameters $\tilde{\theta}$ are chosen to minimize the *objective function* involving the data, based on the *mean squared error* (MSE) between $\hat{\mathbf{y}}_i$ and $\mathbf{y}_i$:

$$\tilde{\theta} = \underset{\theta}{\operatorname{argmin}} \frac{1}{n} \sum_{i=1}^{n} ||\mathbf{y}_i - \hat{\mathbf{y}}_{i;\theta}||_2^2 \tag{4}$$

where $||\cdot||_2$ is the L_2 norm, and $\hat{\mathbf{y}}_{i;\theta}$ is the model approximation of $\mathbf{y}_i$ using parameters θ. The optimal parameters $\tilde{\theta}$ are estimated using an iterative procedure in which an initial guess for the parameter values θ_0 is repeatedly updated according to the gradient of objective function (Equation (4)) with respect to the parameters.

To facilitate training of an ANN, it is convenient to scale the inputs and targets of the model to lie in the same range. We do so by scaling all input and target variables to the interval $[0, 1]$ using the formula:

$$x_{scaled} = \frac{x_{orig} - x_{min}}{x_{max} - x_{min}} \tag{5}$$

where x_{min} and x_{max} are the minimum and maximum of variable x as encountered in the training data.

The ANN model was implemented in Matlab 8.5 (R2015a) using the Neural Network toolbox. This tool is known for the efficient implementation of the Levenberg-Marquardt algorithm to neural network training, which appears to be the fastest method for training moderate-sized feedforward neural networks up to several hundred weights (Hagan et al, 2014). The collected raw data was divided into three sets for training (70%), validation (15%) and test (15%) purposes. The training set is used for computing the gradient and updating the network weights. The validation set provides the basis for optimizing the network setup, and to guard against overfitting the weights on the training set. The test set is used to give an independent verification of the model design (Demuth et al, 2009). To find $\tilde{\theta}$ given the training data, the `lmtrain` optimization method provided with the toolbox was used. This method often finds better (local) optima than regular gradient-descent (and in less iterations) by computing an approximation of the second derivative of the objective function with respect to the parameters, to estimate the stationary points of the gradient, corresponding to the minima of the objective function.

3 Results and discussion

3.1 Experimental data and problem-solving approach

A total of 182 samples were collected from the permeate (i. e. product) stream of the EMR during 10 independent experimental runs. The EMR was operated by varying the residence time and the enzyme load under fixed temperature, pH, and sucrose feed concentration. The total concentration of all carbohydrate fractions was 40 w/w% in the collected samples, containing GF3, GF2, GF, G and F in various composition. The chemical composition and UV spectral data of the samples were obtained via the chromatographic and spectroscopic methods, as described in Sect. "2.4".

The formation of individual compounds in the EMR is governed by certain physical and chemical relationships, and thus, depends on the reaction and operational conditions employed in the EMR. It is to be noted that investigating the influence of operational settings of EMR on FOS production is beyond the scope of this study. Our goal is to obtain a dataset in which the carbohydrate composition varies in a broad range in order to simulate possible scenarios that may occur in real-life applications operating under both optimal and suboptimal conditions. Other reactor configurations, such as packed bed reactors, in which an enzyme-free product stream is produced, are also suitable to generate such a dataset. In this sense, the choice of EMR is arbitrary.

Fig. 2 shows the relative mass percentage of individual saccharides in the samples collected during the experimental phase, sorted in descending order according to the sucrose concentration.

Obviously, an UV absorbance value measured at a single wavelength is not suitable for estimating the relative concentrations of the individual saccharide fractions. However, absorbance values recorded for a range of wavelengths may contain valuable information regarding chemical composition in such a multi-component system. Fig. 3 presents the UV spectra of two illustrative samples and their corresponding composition measured by HPLC.

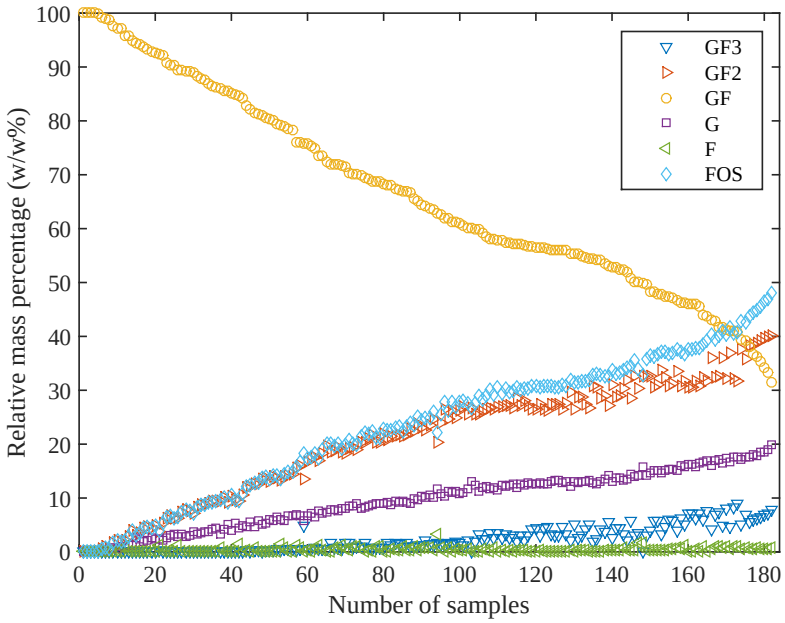

Fig. 2 Relative mass percentage of individual carbohydrate fractions in samples collected from the permeate stream of the enzyme membrane reactor at several settings of residence time and enzyme load. Operation conditions: pH 5.7±0.2, 50±0.5°C, 40 w/w% sucrose feed, 20 kDa UF membrane.

The large deviation observed in the absorption profiles is attributed to the relative ratio of mono-, di-, and oligosaccharides present in the samples. The aim of this study was to find the fundamental relation between the spectra and corresponding saccharides composition. In other words, we want to use the easy-to-measure spectrographs, i. e. absorbance values measured at a given range of wavelengths, to predict the amount of different saccharides in the samples. For this purpose, we employ artificial neural networks.

3.2 Determination of ANN hyperparameters

In terms of hyperparameters, the early stopping criterion and the hidden layer size (i.e. number of neurons in the hidden layer) were investigated for the optimal setting. In preliminary tests we have found, that deeper models (models with multiple hidden lay-

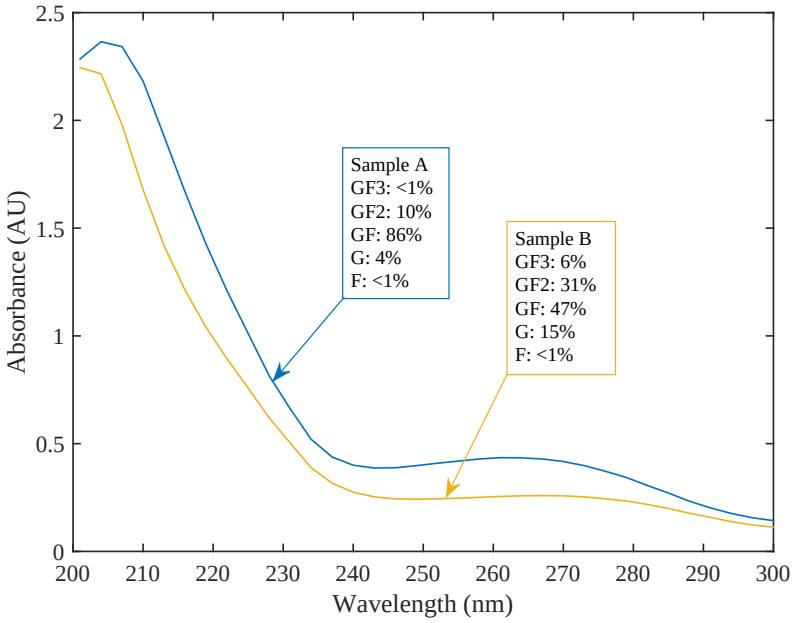

Fig. 3 UV spectra of two illustrative samples and corresponding chemical compositions determined by HPLC.

ers) do not give substantially better results, thus a simple model with a single hidden layer was used in this work for reasons of parsimony. The rest of the model parameters were set to the default values provided in the Neural Network Toolbox version 8.3. The hyperparameters including the training parameters of the Levenberg-Marquardt algorithm are shown in Table 1. Training is stopped when either of the following scenarios take place: the maximum number of training iterations (Max epochs) is reached, the performance goal is achieved, the performance gradient falls below the specified minimum performance gradient, the dampening parameter μ exceeds the specified maximum μ, or the validation error increases for the number of iterations specified by the early stopping criterion.

The early stopping criterion terminates the training of the network after the error on the validation set increases for a specified number of iterations. This prevents the model from adapting to variation in the training set that is due to measurement error

Table 1 Hyperparameters of the final model including the training parameters of the Levenberg-Marquardt algorithm

Parameter	Value
Number of hidden neurons	15
Max epochs	1000
Performance goal	0
Early stopping criterion	50
Minimum performance gradient	1e-7
Initial adaptive value (μ)	0.001
μ decrease factor	0.1
μ increase factor	10
Maximum μ	1e10

and other extraneous influences, and tends to produce models that better generalize beyond the training set. After terminating training, the weights at the minimum of the validation error are returned. Since the decrease of the validation error during training may be non-monotonic, a certain tolerance to increase of validation error is necessary. In our experiments, we found that a tolerance of 50 iterations was enough to make sure that the training was not stopped before the minimum validation error was reached.

Training performance of the models averaged at a determination coefficient of 0.99 and MSE of $<$10 indicating that all of the tested models were capable of learning the underlying function of the training data. To choose the best neural network architecture in terms of the number of neurons in the hidden layer, networks with hidden layer sizes of 1 neuron to 20 neurons were created. Choice of the number of neurons to be examined was based on recommendations from the literature (Panchal et al, 2011; Huang, 2003). At each configuration the network was trained 80 times with random divisions of the data into training and validation. The MSE on the validation set was recorded for every network. The optimal setup was chosen by the average error on the validation set achieved at the different hidden layer sizes. Fig. 4 shows the resulting MSE values on a logaritmic scale for each hidden layer size.

The hidden layer size appeared to have little impact on the validation error in the range 4 to 20 neurons. Nonetheless, the best results were achieved with 15 neurons in

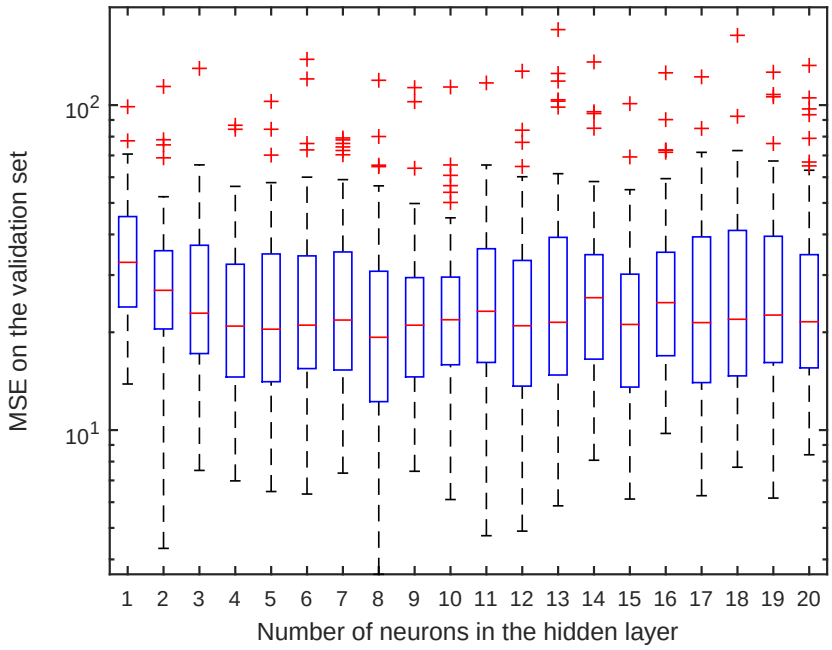

Fig. 4 Boxplot of the MSE on the validation set at different hidden layer sizes on a logaritmic scale.

the hidden layer. Thus, this network architecture was retained to be used for model validation and testing.

3.3 Model performance

The model was validated on the test set, a randomly selected 15% of the data, that was not used in training the network in any way. A determination coefficient of 0.98 with a MSE value of 19.63 was achieved for the test set. Predicted concentration of individual saccharide fractions for the test set (expressed in relative mass percentage) is plotted against the reference values in Fig. 5.

The performance of the model for the test set is shown in detail in Table 2 including the prediction error (MSE), goodness of fit (slope, intercept, R^2) and the F-test (i. e. test for a significant linear regression relationship between the response variable and the predictor variables) results for each component.

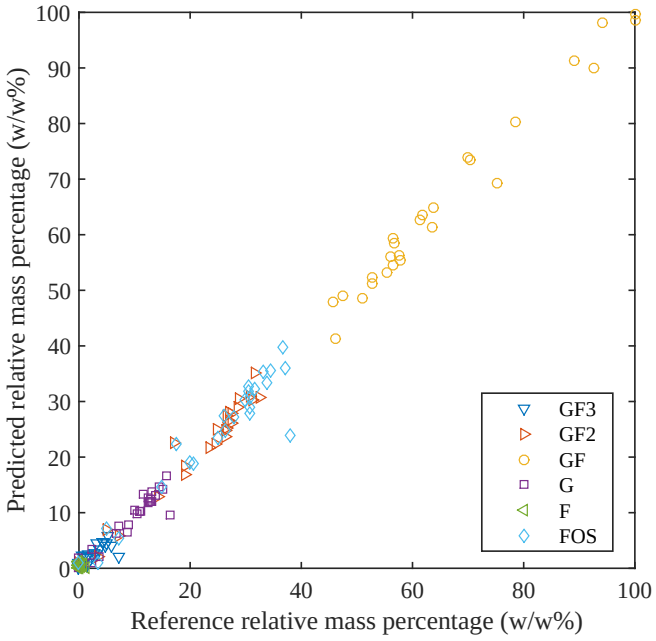

Fig. 5 Predicted versus reference concentration of individual saccharide fractions in the test set

The results indicate that the developed ANN model provides satisfactory performance for the prediction of GF2, GF, G and total FOS. As shown in Table 2, smaller R-squared values were obtained for components in low concentrations (GF3 and F). The reason of the poorer prediction likely originates from the specific features of the reference method. Note that samples were diluted prior to HPLC to avoid exceeding the upper measurement limit of the RI detector. Thus, the main components (GF, GF2, and G), which are present in high concentrations, are measurable. However, the investigated range of concentration for GF3 and F tends to be close to the lower detection limit of the HPLC, resulting relatively imprecise (but otherwise accurate) measurements. For F and GF3, the measurement error relative to the variance of the concentration is much larger, and since the measurement error cannot (and should not) be learned by the model, less accurate predictions are made for those components.

A common way of improving the analysis of compounds in low concentration is to repeat HPLC tests without dilution. This would be, however, a laborious task for

such a large dataset (182 observations). We would like to highlight that the reported ANN predicts F poorly only in relative terms, as measured by the R-squared value. The model predicts its concentrations well in absolute terms, i. e. adequately estimates that its concentration is very low (around 1 w/w%). From the technological point of view, this latter information is more important. As a compromise, we may sacrifice model fit for compounds in low concentration in order to reduce experimental efforts required for model building.

Table 2 Performance of the retained network on the test set by compounds

component	GF3	GF2	GF	G	F	FOS
MSE	1.66	3.40	6.59	2.81	0.32	10.79
slope	0.65	0.98	1.01	0.90	0.06	0.96
intercept	0.81	0.22	-1.29	0.44	0.34	0.56
R^2	0.62	0.97	0.98	0.88	0.08	0.92
F-test	38.3	672	1040	184	0.05	288
p-value	0.00	0.00	0.00	0.00	0.82	0.00

The reference and estimated relative mass percentage values for the test set are shown on Fig 6. The reference values and the estimated values are represented by open and closed symbols, respectively.

Note that the UV-ANN method may also function as an alarm system to detect unwanted disturbances during process run (e. g. microbial contamination, pH shift, temperature and concentration disturbances, etc.) that may occur in real-life applications. However, the system is not able to provide any specific information on the type of disturbance, unless it is previously calibrated for such unwanted scenarios. The here proposed method is general in the sense that it could potentially be applied for any reactor configurations, given that experimental data is available for the specific process environment, and thus, the network can be re-trained following the procedure described in this paper.

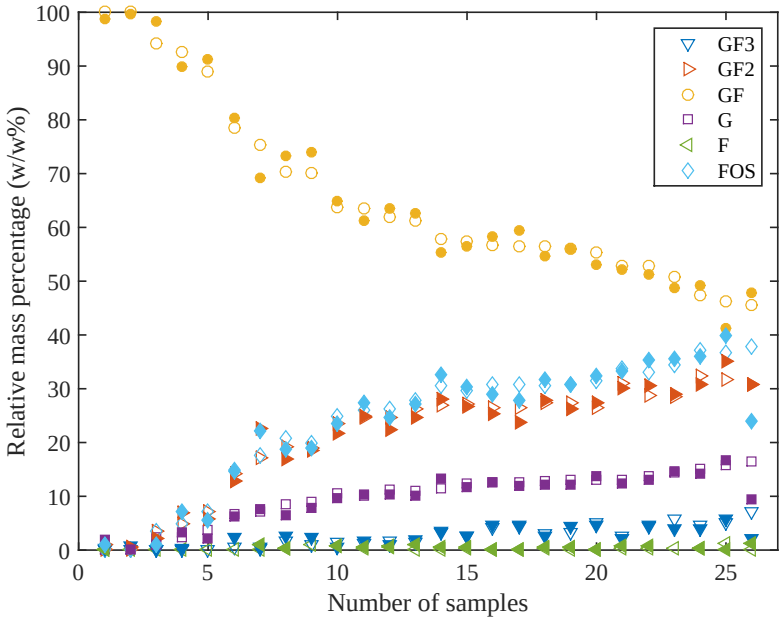

Fig. 6 Reference (open symbols) and predicted (closed symbols) concentrations of individual saccharide fractions in the test set.

4 Conclusions

In conclusion, our results suggest that the proposed UV-ANN method has a great potential to be applied as an on-line monitoring tool in FOS manufacturing processes. It provides satisfactory estimation of the main components found in the product stream of enzymatic FOS production. The estimation accuracy is suitable for tracing the course of the bioconversion. It may be implemented at certain critical points of the FOS production line to monitor the progress of the reaction and to detect possible failures and disturbances in the operation.

Acknowledgements

The preparation of this work was supported by the Marie Skłodowska-Curie grant of the EU FP7 Framework Programme (PCIG11-GA-2012-322219) and the Bolyai Scholarship Programme of the Hungarian Academy of Sciences.

References

Bali V, Panesar PS, Bera MB, Panesar R (2013) Fructo-oligosaccharides: Production, purification and potential applications. Critical reviews in food science and nutrition 8398(June 2014):37–41, DOI 10.1080/10408398.2012.694084, URL http://www.ncbi.nlm.nih.gov/pubmed/24915337

Barclay T, Ginic-Markovic M, Johnston MR, Cooper PD, Petrovsky N (2012) Analysis of the hydrolysis of inulin using real time 1H NMR spectroscopy. Carbohydrate Research 352:117–125, DOI 10.1016/j.carres.2012.03.001, URL http://dx.doi.org/10.1016/j.carres.2012.03.001

Borromei C, Careri M, Cavazza A, Corradini C, Elviri L, Mangia A, Merusi C (2009) Evaluation of Fructooligosaccharides and Inulins as Potentially Health Benefiting Food Ingredients by HPAEC-PED and MALDI-TOF MS. International journal of analytical chemistry 2009:530,639, DOI 10.1155/2009/530639

Cámara M, Torrecilla JS, Caceres JO, Cortes Sánchez Mata M, Fernandez-Ruiz V (2010) Neural network analysis of spectroscopic data of lycopene and β-carotene content in food samples compared to HPLC-UV-Vis. Journal of Agricultural and Food Chemistry 58(1):72–75, DOI 10.1021/jf902466x

Chen SC, Sheu DC, Duan KJ (2014) Production of fructooligosaccharides using β-fructofuranosidase immobilized onto chitosan-coated magnetic nanoparticles. Journal of the Taiwan Institute of Chemical Engineers 45(4):1105–1110, DOI 10.1016/j.jtice.2013.10.003, URL http://dx.doi.org/10.1016/j.jtice.2013.10.003

Corradini C, Bianchi F, Matteuzzi D, Amoretti A, Rossi M, Zanoni S (2004) High-performance anion-exchange chromatography coupled with pulsed amperometric de-

tection and capillary zone electrophoresis with indirect ultra violet detection as powerful tools to evaluate prebiotic properties of fructooligosaccharides and inulin. Journal of Chromatography A 1054(1-2):165–173, DOI 10.1016/j.chroma.2004.07.109

Corradini C, Lantano C, Cavazza A (2013) Innovative analytical tools to characterize prebiotic carbohydrates of functional food interest. Analytical and Bioanalytical Chemistry 405(13):4591–4605, DOI 10.1007/s00216-013-6731-6

Demuth H, Beale M, Hagan M (2009) Neural Network Toolbox^{TM} 6 User's Guide, Revised for Version 6.0.3 (Release 2009b)

Dias LG, Veloso ACA, Correia DM, Rocha O, Torres D, Rocha I, Rodrigues LR, Peres AM (2009) UV spectrophotometry method for the monitoring of galacto-oligosaccharides production. Food Chemistry 113(1):246–252, DOI 10.1016/j.foodchem.2008.06.072, URL http://dx.doi.org/10.1016/j.foodchem.2008.06.072

Dominguez AL, Rodrigues LR, Lima NM, Teixeira JA (2013) An Overview of the Recent Developments on Fructooligosaccharide Production and Applications. Food and Bioprocess Technology pp 1–14, DOI 10.1007/s11947-013-1221-6

Falguera V, Aliguer N, Falguera M (2012) An integrated approach to current trends in food consumption : Moving toward functional and organic products? Food Control 26(2):274–281, DOI 10.1016/j.foodcont.2012.01.051, URL http://dx.doi.org/10.1016/j.foodcont.2012.01.051

Ghazi I, Gómez De Segura A, Fernández-Arrojo L, Alcalde M, Yates M, Rojas-Cervantes ML, Plou FJ, Ballesteros A (2005) Immobilisation of fructosyltransferase from Aspergillus aculeatus on epoxy-activated Sepabeads EC for the synthesis of fructo-oligosaccharides. Journal of Molecular Catalysis B: Enzymatic 35(1-3):19–27, DOI 10.1016/j.molcatb.2005.04.013

Grube M, Bekers M, Upite D, Kaminska E (2002) Infrared spectra of some fructans. Spectroscopy 16(3-4):289–296, DOI 10.1155/2002/637587, URL http://www.hindawi.com/journals/jspec/2002/637587/abs/

Hagan M, Demuth H, Beale M, De Jesús O (2014) Neural network design. Martin Hagan

Hicke HG, Becker M, Paulke BR, Ulbricht M (2006) Covalently coupled nanoparticles in capillary pores as enzyme carrier and as turbulence promoter to facilitate enzymatic polymerizations in flow-through enzyme-membrane reactors. Journal of Membrane Science 282(1-2):413–422, DOI 10.1016/j.memsci.2006.05.051

Huang GB (2003) Learning capability and storage capacity of two-hidden-layer feedforward networks. IEEE Transactions on Neural Networks 14(2):274–281, DOI 10.1109/TNN.2003.809401

Joye D, Hoebregs H (2000) Determination of oligofructose, a soluble dietary fiber, by high-temperature capillary gas chromatography. Journal of AOAC International 83(4):1020–1025

Kovács Z, Benjamins E, Grau K, Ur Rehman A, Ebrahimi M, Czermak P (2014) Recent Developments in Manufacturing Oligosaccharides with Prebiotic Functions. In: Zorn H, Czermak P (eds) Biotechnology of Food and Feed Additives, Springer Berlin Heidelberg, Berlin, Heidelberg, pp 257–295, DOI 10.1007/10.2013.237, URL http://dx.doi.org/10.1007/10_2013_237

Li J, Liu X, Zhou B, Zhao J, Li S (2013) Determination of fructooligosaccharides in burdock using HPLC and microwave-assisted extraction. Journal of Agricultural and Food Chemistry 61(24):5888–5892, DOI 10.1021/jf400534n

Lin H, Zhao J, Sun L, Chen Q, Zhou F (2011) Freshness measurement of eggs using near infrared (NIR) spectroscopy and multivariate data analysis. Innovative Food Science and Emerging Technologies 12(2):182–186, DOI 10.1016/j.ifset.2011.01.008, URL http://dx.doi.org/10.1016/j.ifset.2011.01.008

Lorenzoni ASG, Aydos LF, Klein MP, Ayub MAZ, Rodrigues RC, Hertz PF (2015) Continuous production of fructooligosaccharides and invert sugar by chitosan immobilized enzymes: Comparison between in fluidized and packed bed reactors. Journal of Molecular Catalysis B: Enzymatic 111:51–55, DOI 10.1016/j.molcatb.2014.11.002

Mateo F, Gadea R, Mateo EM, Jiménez M (2011) Multilayer perceptron neural networks and radial-basis function networks as tools to forecast accumulation of deoxynivalenol in barley seeds contaminated with Fusarium culmorum. Food Control 22(1):88–95, DOI 10.1016/j.foodcont.2010.05.013, URL http://dx.doi.org/10.1016/j.foodcont.2010.05.013

Mutanda T, Mokoena MP, Olaniran AO, Wilhelmi BS, Whiteley CG (2014) Microbial enzymatic production and applications of short-chain fructooligosaccharides and inulooligosaccharides: Recent advances and current perspectives. Journal of Industrial Microbiology and Biotechnology 41(6):893–906, DOI 10.1007/s10295-014-1452-1

Nguyen QD, Rezessy-Szabó JM, Czukor B, Hoschke Á (2011) Continuous production of oligofructose syrup from Jerusalem artichoke juice by immobilized endo-inulinase. Process Biochemistry 46(1):298–303, DOI http://dx.doi.org/10.1016/j.procbio.2010.08.028, URL http://www.sciencedirect.com/science/article/pii/S1359511310003399

Nishizawa K, Nakajima M, Nabetani H (2000) A forced-flow membrane reactor for transfructosylation using ceramic membrane. Biotechnology and Bioengineering 68(1):92–97, DOI 10.1002/(SICI)1097-0290(20000405)68:1<92::AID-BIT11>3.0.CO;2-1

Panchal G, Ganatra A, Kosta Y, Panchal D (2011) Behaviour analysis of multilayer perceptrons with multiple hidden neurons and hidden layers. International Journal of Computer Theory and Engineering 3(2):332–337, URL http://www.ijcte.org/papers/328-L318.pdf

Petkova N, Denev P (2015) Methods for determination of inulin. In: Hadzhiev B (ed) Monograph of 4rd European Young Engineers Conference 2015, Food Research & Development Institute, Plovdiv, UFT Academic Publishing House, Plovdiv, Plovdiv, Bulgaria, ISSN 2367-6213, p 135

Petkova N, Radka V, Denev P, Ivanov I, Pavlov A (2014) HPLC-RID method for determination of inulin and fructooligosaccharides. Acta Scientifica Naturalis 1:99–107

Prabhu AA, Jayadeep A (2017) Optimization of enzyme-assisted improvement of polyphenols and free radical scavenging activity in red rice bran: A statistical and neural network-based approach. Preparative Biochemistry and Biotechnology 47(4):397–405, DOI 10.1080/10826068.2016.1252926, URL https://www.tandfonline.com/doi/full/10.1080/10826068.2016.1252926

Rastall RA (2010) Functional Oligosaccharides: Application and Manufacture. Annual Review of Food Science and Technology 1:305–339, DOI 10.1146/annurev.food.080708.100746

Sarup R, Pal R, Kennedy JF (2016) International Journal of Biological Macromolecules Recent insights in enzymatic synthesis of fructooligosaccharides from inulin. International Journal of Biological Macromolecules 85:565–572, DOI 10.1016/j.ijbiomac.2016.01.026, URL http://dx.doi.org/10.1016/j.ijbiomac.2016.01.026

Tanriseven A, Aslan Y (2005) Immobilization of pectinex ultra sp-l to produce fructooligosaccharides. Enzyme and Microbial Technology 36(4):550 – 554, DOI http://dx.doi.org/10.1016/j.enzmictec.2004.12.001, URL http://www.sciencedirect.com/science/article/pii/S014102290400362X

Ur Rehman A, Kovacs Z, Quitmann H, Ebrahimi M, Czermak P (2016) Enzymatic production of fructo-oligosaccharides from inexpensive and abundant substrates using a membrane reactor system. Separation Science and Technology 6395(April):01496,395.2016.1167,740, DOI 10.1080/01496395.2016.1167740, URL http://www.tandfonline.com/doi/full/10.1080/01496395.2016.1167740

Van Den Broeke J, Langergraber G, Weingartner A (2006) On-line and in-situ UV/vis spectroscopy for measurements: a brief review. Spectroscopy Europe 1 18(4):4–7

Veloso ACA, Rodrigues LR, Dias LG, Peres AM (2012) Chapter 14 uv spectrophotometry method for dietary sugars. In: Dietary Sugars: Chemistry, Analysis, Function and Effects, The Royal Society of Chemistry, pp 229–248, DOI 10.1039/9781849734929-00229, URL http://dx.doi.org/10.1039/9781849734929-00229